Chinese Chemical Letters 36 (2025) 110337

Contents lists available at ScienceDirect

Chinese Chemical Letters

journal homepage: www.elsevier.com/locate/cclet

Polystyrene-supported phosphoric-acid catalyzed atroposelective construction of axially chiral *N*-aryl benzimidazoles

Chengyao Zhao[a,1], Jingyuan Liao[a,1], Yuxiang Zhu[b], Yiying Zhang[c], Lianjie Zhai[c,*], Junrong Huang[a,*], Hengzhi You[a,d,*]

[a] School of science, Harbin Institute of Technology (Shenzhen), Shenzhen 518055, China
[b] School of Pharmaceutical Sciences (Shenzhen), Shenzhen Campus of Sun Yat-sen University, Shenzhen 518107, China
[c] State Key Laboratory of Fluorine & Nitrogen Chemicals, Xi'an Modern Chemistry Research Institute, Xi'an 710069, China
[d] Green Pharmaceutical Engineering Research Center, Harbin Institute of Technology (Shenzhen), Shenzhen 518055, China

ARTICLE INFO

Article history:
Received 11 March 2024
Revised 29 July 2024
Accepted 12 August 2024
Available online 13 August 2024

Keyword:
Asymmetric catalysis
Heterogeneous catalysis
Chiral phosphoric acid
Atroposelective synthesis
N-Aryl benzimidazoles

ABSTRACT

The significance of axial chiral compounds in asymmetric organic catalysis, functional materials, and pharmaceutical useful molecules has encouraged advancements in the atroposelective synthesis of such compounds. Herein, we report the first atroposelective construction of axially chiral *N*-aryl benzimidazoles catalyzed by a polymer-supported chiral phosphoric acid. A varied library of atropisomers has been synthesized in 30%-96% yield with 58%-98% enantiomeric excess (*ee*) under a straightforward reaction setup (without the use of molecular sieves). Notably, even after 12 cycles, the immobilized catalyst maintained its reactivity and selectivity (TON > 540).

N-Aryl benzimidazoles, serving as a pivotal core, are prevalent in a multitude of biologically and pharmacologically active compounds [1,2]. The distinct pharmacological activities are attributed to their atropisomerism, including RXR partial agonist [3] and PI3Kβ inhibitor [4,5]. Additionally, they serve as functional materials in the field of organic synthesis and pharmaceutical chemistry, such as chiral ligand Biminap [6] and chiral derivatizing agent (Fig. 1) [7]. The enantioselective synthesis of *N*-aryl benzimidazole atropisomers remained undeveloped until 2019, when the first atroposelective synthesis of these compounds was achieved by the Miller group (Fig. 2a) [8]. Their approach involved the use of chiral phosphoric acids (CPAs) or peptide-based phosphoric acids to catalyze an enantioselective cyclodehydration process between the amide and amine derivatives, producing the axially chiral *N*-aryl benzimidazoles. Subsequently, several research groups have developed new approaches for the atroposelective construction of *N*-aryl benzimidazoles. The Fu group [9] redesigned and developed a CPA-catalyzed carbon-carbon bond cleavage approach (Fig. 2b), while the Liu group [10] reported the first Pd-catalyzed intramolecular cross-coupling strategy (Fig. 2c). Later, the Tan group [11] developed a novel CPA-catalyzed ring formation approach using nitrosobenzene (Fig. 2d).

As in earlier advancements, homogeneous CPAs occupy a leading position in the asymmetric synthesis of *N*-aryl benzimidazoles. However, the use of homogeneous catalyst protocols presents considerable challenges for future industrial applications due to their high costs, high catalyst loading (5–20 mol%), complex purification processes, and recyclability issue. To overcome these drawbacks, the immobilization of CPAs became a practical and advantageous alternative. In 2010, Rueping group demonstrated the first immobilization of CPAs by copolymerization [12]. Since then, the immobilization of CPAs has garnered extensive attention and has undergone significant development over the past decade [13–17]. Meanwhile, the application of immobilized CPAs in asymmetric synthesis has been well explored, including asymmetric hydrogenation [13], asymmetric allylation [18], asymmetric cyclization [19], asymmetric dearomatization [15] and desymmetrization [20]. However, to the best of our knowledge, atroposelective construction of *N*-aryl benzimidazoles using immobilized CPAs has not been developed. Styrene copolymerization is one of the most robust strategies to achieve catalyst immobilization, and our group has previously applied this approach to the immobilization of BINOL-derivative ligands [21]. Moreover, polystyrene support will provide a hydrophobic microenvironment for the catalytic sites [22–24], which may accelerate the reaction and avoid the use of additives like

* Corresponding authors.
E-mail addresses: trihever0210@126.com (L. Zhai), hjunrong@hit.edu.cn (J. Huang), youhengzhi@hit.edu.cn (H. You).
[1] These authors contributed equally to this work.

https://doi.org/10.1016/j.cclet.2024.110337
1001-8417/

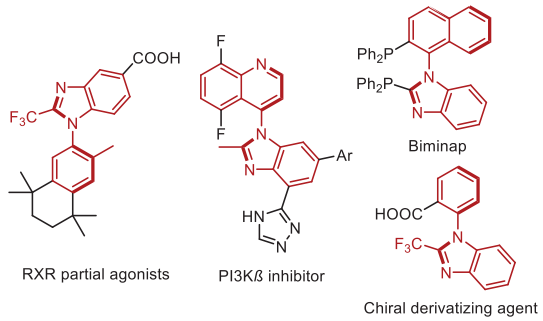

Fig. 1. Representative biologically active compounds and functional materials.

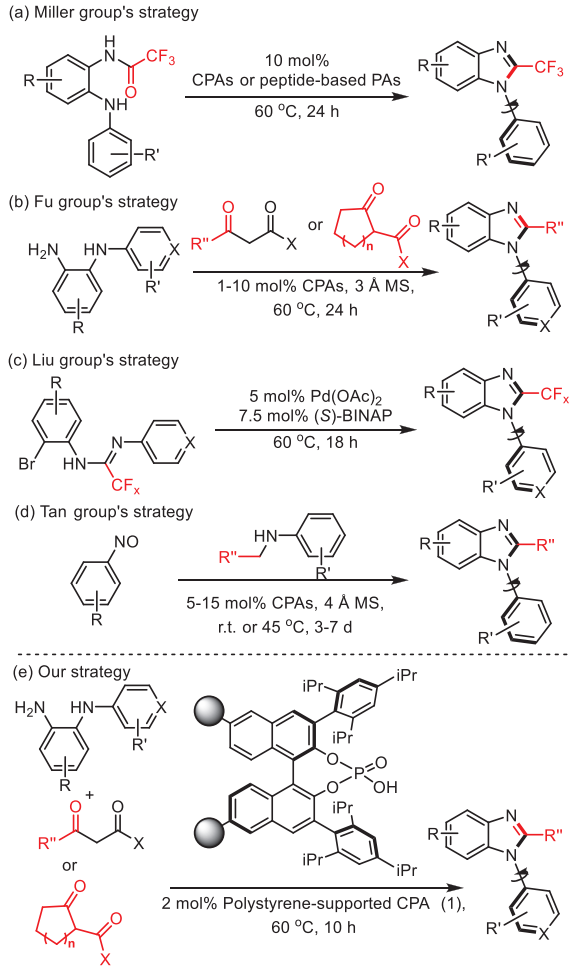

Fig. 2. Atroposelective construction of axially chiral *N*-aryl benzimidazoles.

molecular sieves. Therefore, we decided to develop a polystyrene-supported CPA catalyst for the atroposelective construction of *N*-aryl benzimidazoles.

In this communication, we report the synthesis of polystyrene-supported CPA **1** and the first atroposelective construction of axially chiral *N*-aryl benzimidazoles using an immobilized CPA catalyst (Fig. 2e). This immobilized catalyst **1**, offers products in high yield and excellent enantioselectivity without the use of molecular sieves, representing a more straightforward reaction setup.

Table 1
Reaction optimization of the atroposelective construction with **2a** and **3a** using immobilized catalyst **1**.[a]

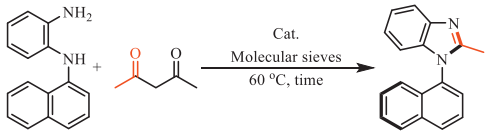

2a **3a** **4aa**

Entry	Cat.	Cat. loading (x mol%)	Time (h)	Solvent	Yield (%)[b]	*ee* (%)[c]
1	TRIP	10	20	Toluene	88	95
2	**1**	10	20	Toluene	91	96
3	**1**	10	20	MeOH	12	20
4	**1**	10	20	MeCN	45	30
5	**1**	10	20	EtOAc	80	93
6	**1**	10	20	DCM	61	89
7	**1**	10	20	Hexane	76	91
8	**1**	5	20	Toluene	91	96
9	**1**	2	20	Toluene	91	96
10	**1**	1	20	Toluene	62	95
11	**1**	1	40	Toluene	64	95
12	**1**	0.5	20	Toluene	57	95
13	**1**	2	10	Toluene	91	96
14	**1**	2	5	Toluene	68	96
15	**1**[d]	2	20	Toluene	90	96
16	TRIP[d]	10	20	Toluene	78	82

[a] Reaction conditions: **2a** (0.1 mmol), **3a** (0.2 mmol), catalyst (x mol%) and solvent (1.5 mL) were stirred in a sealed vial at 60 °C under an Ar atmosphere for a given time.
[b] Isolated yield.
[c] The *ee* values were determined by HPLC analysis on a chiral stationary phase using a Daicel Chiralpak AD-H or ID column.
[d] Without molecular sieves.

The synthesis of catalyst **1** was based on a modified procedure from our previous report [21], which commenced with the bromination of a BINOL derivative bearing two tris-isopropyl benzene substituents. This was followed by Suzuki-coupling, copolymerization, phosphorylation, and hydrolysis to give the CPA catalyst **1** in 65% overall yield. The structural integrity and materials morphology of the catalyst **1** were characterized by solid-state nuclear magnetic resonance (NMR), X-ray photoelectron spectroscopy (XPS), inductively coupled plasma optical emission spectrometry (ICP-OES), transmission electron microscopy (TEM) and energy-dispersive X-ray spectrometer (EDS) in detail. The solid-state ^{13}C NMR spectrum of **1** exhibited connected peaks ranging from 120 ppm to 160 ppm, which are assigned to the aromatic carbons, and from 10 ppm to 50 ppm, assigned to the isopropyl carbons, respectively (Fig. 3a). In the solid-state ^{31}P NMR spectrum of **1**, only one broad peak at 4.12 ppm was observed, which is similar to the characteristic signal of the chiral phosphoric acid monomer (TRIP) at 1.5 ppm (Fig. 3b). Furthermore, similar P 2p peak signals were observed for **1** and TRIP in the XPS spectra (132.8 *vs.* 133.5 eV, Fig. 3c). The ICP-OES analysis showed that the P content in **1** is 0.48% (see Supporting information for details), which revealed the TRIP loading to be 95% (theoretical P content is 0.50%). TEM images showed that **1** consisted of sphere particles with diameters of 100 nm (Fig. 3d). The location of TRIP at **1** was verified by TEM-EDS overlap map, which indicated that the elements C, O and P are uniformly distributed in the solid matrix (Fig. 3e). All these results suggest that the chemical structure and properties of the phosphoric acid were well retained after immobilization.

Having synthesized the polystyrene-supported CPA, we then proceeded to investigate the reactivity and atroposelectivity of the catalyst by using N^1-(naphthalen-1-yl)benzene-1,2-diamine (**2a**) and acetylacetone (**3a**) as the model substrates. Our investigation began with reaction optimization (Table 1). In comparison to ho-

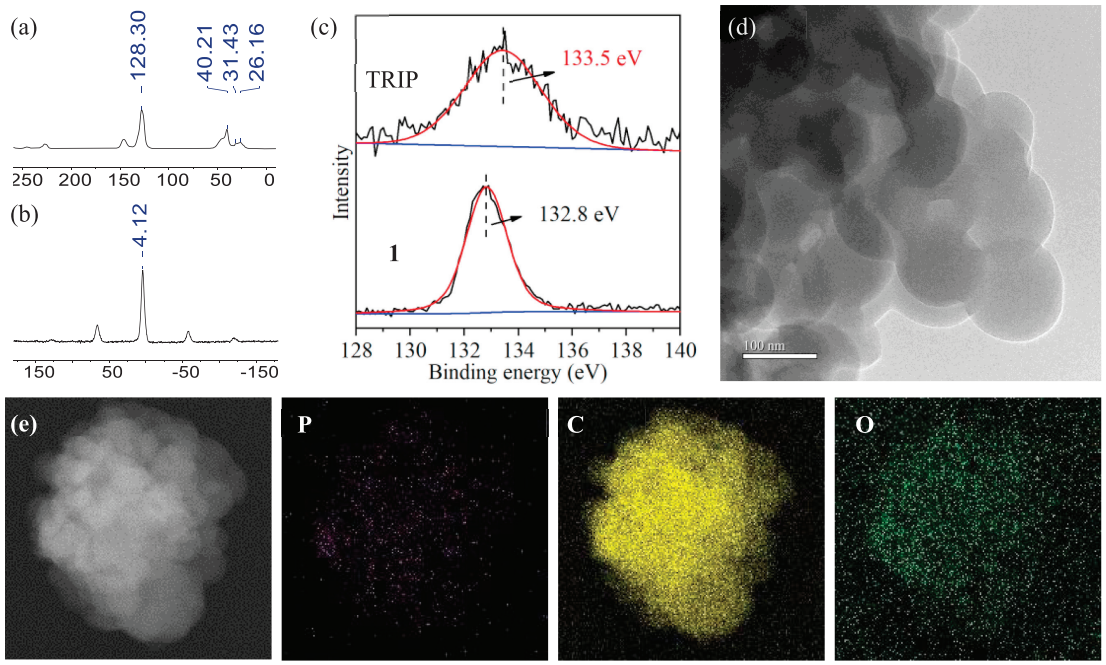

Fig. 3. Characterizations of the solid catalyst. (a) Solid-state ^{13}C NMR spectrum of **1**. (b) Solid-state ^{31}P NMR spectrum of **1**. (c) XPS spectra of TRIP and **1**. (d) TEM and (e) EDS mapping images of **1**.

mogeneous TRIP catalyst (entry 1, 88% yield with 92% *ee* [9]), the reaction using **1** exhibited greater efficiency, yielding the target compound **4aa** in 91% isolated yield with 96% *ee* (entry 2). Given that the swelling ability of the supported catalyst in different solvents significantly impacts its performance [25], we next investigated the solvent effect. The employment of polar protic solvent MeOH was harmful, giving the product in 12% yield with 20% *ee* (entry 3). Subsequently, three different types of polar aprotic solvents were evaluated but only unsatisfactory results were obtained (entries 4–6). Performing the reaction in a less swelling nonpolar solvent hexane produced compound **4aa** with a 91% *ee*, albeit with a diminished yield (entry 7). Leveraging the high efficiency of **1**, we successfully reduced the catalyst loading to 2 mol% without compromising on catalytic performance (entries 8 and 9). Further lowering the catalyst loading (0.5 or 1 mol%) provoked a decrease in yield but left the enantioselectivity undamaged (entries 10 and 12). Attempt to improve yield by extending the reaction time proved unsuccessful (entry 11). As expected, the heterogeneous catalyst **1** could work smoothly without the molecular sieves (90% yield and 96% *ee*, entry 15). This can be attributed to the hydrophobicity of the polystyrene support, which encourages the formation of the imine intermediate by facilitating the removal of water molecules. In contrast, the homogeneous TRIP catalyst suffered a roughly 10% loss in both yield and *ee* (entry 16). Therefore, these optimal conditions (2 mol% of **1** in toluene at 60 °C without molecular sieves) were used in further studies.

Next, we explored the versatility of this immobilized catalyst **1** by varying substituents on the benzene ring of the substrate **2** (Scheme 1), including 4-methyl, 4-fluoro, 4–chloro, 4–bromo, 6–chloro, and 5–methoxy substituents (**2d**-**2g**). Additionally, we also examined the substrate bearing a *N*-heterocyclic group instead of a naphthalene (**2h**). Regarding the scope of the multicarbonyl compounds **3**, we chose three β-dicarbonyl compounds (**3a**, **3b**, **3c**), dimethyl 1,3-acetonedicarboxylate (**3d**), and three cyclic β-dicarbonyl compounds (**3e**, **3f**, **3g**). Comparison of yield and *ee* between our immobilized CPA catalyst and homogeneous TRIP [9] catalyst was also included (Fig. 4).

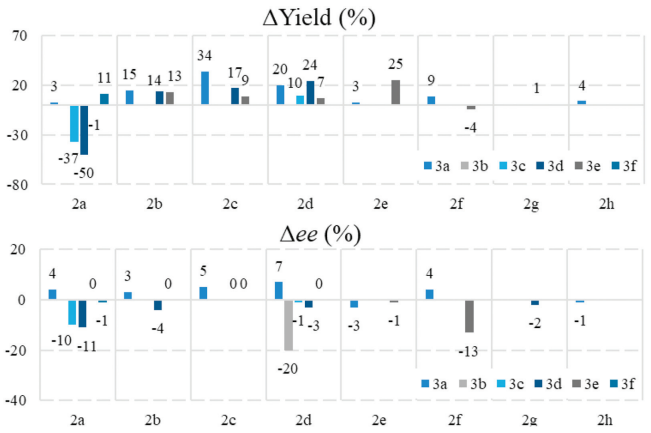

Fig. 4. Comparison of the catalytical efficiency between TRIP and **1**, the data of TRIP are from the literature [9].

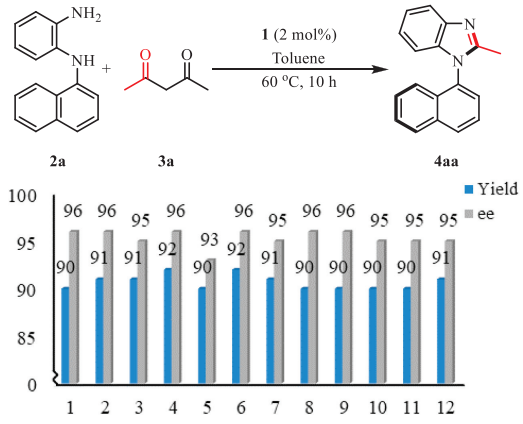

Fig. 5. Recycling of **1** for the atroposelective construction of axially chiral *N*-aryl benzimidazole **4aa**.

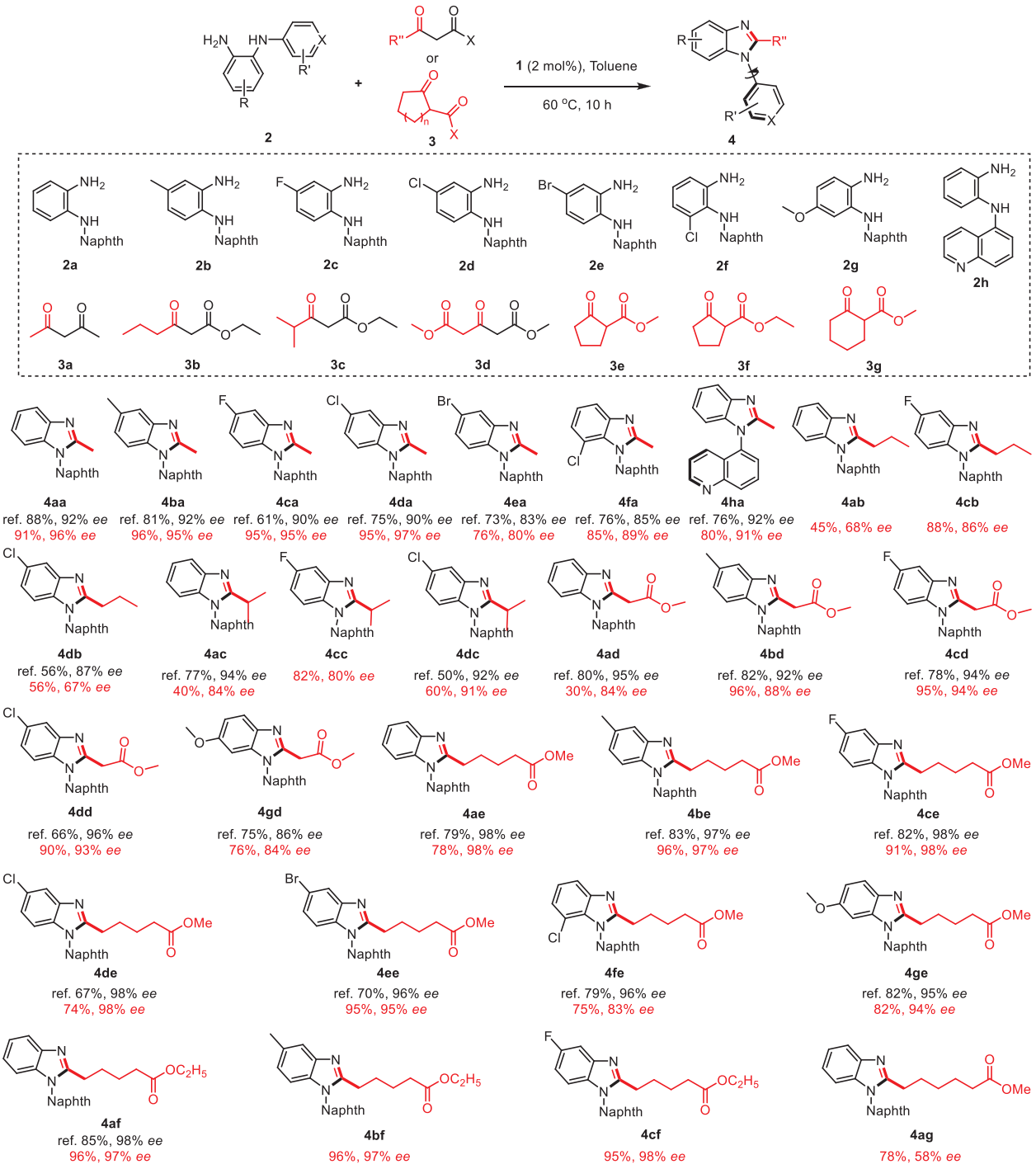

Scheme 1. Scope of N^1-(aryl)benzene-1,2-diamines **2** and multicarbonyl compounds **3** in the atroposelective construction of axially chiral *N*-aryl benzimidazoles.

The Δyield and Δ*ee* mean the difference between employing **1** and TRIP as catalyst. The results suggest that the yield is generally higher (average value of Δyield = 5.8%) and the *ee* (average value of Δ*ee* = −2.1%) is comparable by using **1** as the catalyst. Most reactions proceeded efficiently with excellent yields and enantioselectivities (up to 95% yield, 98% *ee*). There were only a few special cases, where the yield or *ee* value conspicuous decreased (**4ac**, **4ad**, **4db**, and **4fe**). The recycling stability of the catalyst **1** was also investigated. After the completion of the reaction, the heterogeneous catalyst **1** could be separated from the reaction mixture *via* simple filtration, followed by washing with dichloromethane until no signal was detected in the TLC analysis. It is noteworthy that before the next run, the recovered catalyst **1** needs to be dried in a vacuum oven at 60 °C for 24 h. With this approach, we have achieved consistent yields and *ee* even after 12 cycles, enabling the production of compound **4aa** with a cumulative TON of 540 (Fig. 5).

In conclusion, polystyrene-supported CPA **1** has been successfully synthesized and thoroughly characterized, spanning from chemical structure to materials morphology. This catalyst demonstrated efficient catalytic ability in the atroposelective construction of axially chiral *N*-aryl benzimidazoles for the first time. A

diverse library of atropisomers has been synthesized, achieving yields ranging from 30% to 96% with ee values between 58% and 98%. In addition, the catalyst maintained its reactivity and selectivity even after 12 cycles (TON $>$ 540).

Declaration of competing interest

The authors declare that they have no known competing financial interests or personal relationships that could have appeared to influence the work reported in this paper.

CRediT authorship contribution statement

Chengyao Zhao: Writing – review & editing, Investigation. **Jingyuan Liao:** Writing – review & editing, Writing – original draft, Investigation, Conceptualization. **Yuxiang Zhu:** Writing – review & editing, Writing – original draft. **Yiying Zhang:** Writing – review & editing. **Lianjie Zhai:** Writing – review & editing, Supervision, Conceptualization. **Junrong Huang:** Writing – review & editing, Writing – original draft, Supervision, Project administration, Funding acquisition, Conceptualization. **Hengzhi You:** Writing – review & editing, Writing – original draft, Supervision, Project administration, Funding acquisition, Conceptualization.

Acknowledgments

This work was supported by Shenzhen Science and Technology Research (Nos. JSGG20201103153807021, GXWD202208 11173736002, KCXFZ20230731094904009). We are also grateful to the Fundamental Research Funds for the Central Universities, Sun Yat-sen University (No. 24qnpy060), Natural Science Foundation of Guangdong Province (No. 2021A1515110366), National Natural Science Foundation of China (Nos. 22302048, 82204231, 22275146) and Shenzhen Key Laboratory of Advanced Functional Carbon Materials Research and Comprehensive Application.

Supplementary materials

Supplementary material associated with this article can be found, in the online version, at doi:10.1016/j.cclet.2024.110337.

References

[1] Y. Bansal, O. Silakari, Bioorg. Med. Chem. 20 (2012) 6208–6236.
[2] Salahuddin, M. Shaharyar, A. Mazumder, Arab. J. Chem. 10 (2017) S157–S173.
[3] F. Ohsawa, S. Yamada, N. Yakushiji, et al., J. Med. Chem. 56 (2013) 1865–1877.
[4] S. Perreault, F. Arjmand, J. Chandrasekhar, et al., ACS Med. Chem. Lett. 11 (2020) 1236–1243.
[5] J. Chandrasekhar, R. Dick, J.Van Veldhuizen, et al., J. Med. Chem. 61 (2018) 6858–6868.
[6] I. Abdellah, N. Debono, Y. Canac, L. Vendier, R. Chauvin, Chem. Asian J. 5 (2010) 1225–1231.
[7] M. Kriegelstein, D. Profous, A. Lyčka, et al., J. Org. Chem. 84 (2019) 11911–11921.
[8] Y. Kwon, J. Li, J.P. Reid, et al., J. Am. Chem. Soc. 141 (2019) 6698–6705.
[9] N. Man, Z. Lou, Y. Li, et al., Org. Lett. 22 (2020) 6382–6387.
[10] P. Zhang, X.M. Wang, Q. Xu, et al., Angew. Chem. Int. Ed. 60 (2021) 21718–21722.
[11] Q.J. An, W. Xia, W.Y. Ding, et al., Angew. Chem. Int. Ed. 60 (2021) 24888–24893.
[12] M. Rueping, E. Sugiono, A. Steck, T. Theissmann, Adv. Synth. Catal. 352 (2010) 281–287.
[13] D.S. Kundu, J. Schmidt, C. Bleschke, A. Thomas, S. Blechert, Angew. Chem. Int. Ed. 51 (2012) 5456–5459.
[14] W. Gong, X. Chen, H. Jiang, et al., J. Am. Chem. Soc. 141 (2019) 7498–7508.
[15] X.Y. Huang, Q. Zheng, L.M. Zou, et al., ACS Catal. 12 (2022) 4545–4553.
[16] S. Li, J. Zhang, S. Chen, X. Ma, J. Catal. 416 (2022) 139–148.
[17] M.B. Chaudhari, P. Gupta, P. Llanes, M.A. Pericàs, Adv. Synth. Catal. 365 (2023) 527–534.
[18] L. Clot-Almenara, C. Rodriguez-Escrich, L. Osorio-Planes, M.A. Pericas, ACS Catal. 6 (2016) 7647–7651.
[19] B. Zhang, L. Shi, R. Guo, Catal. Lett. 145 (2015) 1718–1723.
[20] J. Lai, M. Fianchini, M.A. Pericàs, ACS Catal. 10 (2020) 14971–14983.
[21] J. Wang, J. Li, Y. Wang, et al., ACS Catal. 12 (2022) 9629–9637.
[22] Y. Huang, L. Yang, M. Huang, et al., Particuology 22 (2015) 128–133.
[23] B. Altava, M.I. Burguete, E. García-Verdugo, S.V. Luis, Chem. Soc. Rev. 47 (2018) 2722–2771.
[24] T. Kitanosono, F. Lu, K. Masuda, Y. Yamashita, S. Kobayashi, Angew. Chem. Int. Ed. 61 (2022) e202202335.
[25] M. Heitbaum, F. Glorius, I. Escher, Angew. Chem. Int. Ed. 45 (2006) 4732–4762.